

Multi messenger astronomy and CTA: TeV cosmic rays and electrons

Piergiorgio Picozza^{a,b}, Mirko Boezio^c

^a*INFN, Sezione di Rome “Tor Vergata”, I-00133 Rome, Italy*

^b*University of Rome “Tor Vergata”, Department of Physics, I-00133 Rome, Italy*

^c*INFN, Sezione di Trieste, I-34149 Trieste, Italy*

Abstract

Cosmic rays are a sample of solar, galactic and extragalactic matter. Their origin and properties are one of the most intriguing question in modern astrophysics. The most energetic events and active objects in the Universe: supernovae explosion, pulsars, relativistic jets, active galactic nuclei, have been proposed as sources of cosmic rays although unambiguous evidences have still to be found. Electrons, while comprising $\sim 1\%$ of the cosmic radiation, have unique features providing important information regarding the origin and propagation of cosmic rays in the Galaxy that is not accessible from the study of the cosmic-ray nuclear components due to their differing energy-loss processes. In this paper we will analyse, discussing the experimental uncertainties and challenges, the most recent measurements on cosmic-ray nuclei and, in particular, electrons with energies from tens of GeV into the TeV region.

Keywords: Cosmic rays, Acceleration of particles, Abundances

1. Introduction

Cosmic rays are a sample of solar, galactic and extragalactic matter which includes all known nuclei and their isotopes, as well as electrons, positrons, and antiprotons. They are associated with the most energetic events and active objects in the Universe: supernovae explosion, pulsars, relativistic jets, active galactic nuclei, although an unambiguous proof of their origin has not until now been found. The measurement of all particle cosmic ray energy spectrum, shown in Fig. 1, ranges for about 32 orders of magnitude in flux determination and more than 21 in explored energy. Three features appear in the spectrum, a first knee at an energy of 3 PeV, a second knee at about 0.5 EeV and an ankle beyond 10 EeV. In this spectrum there are, quite hidden, the answers to the main questions in the cosmic rays research. Where do the particles are coming from? How and where they are getting accelerated? How do they propagate through the interstellar medium and what kind of interaction do they encounter? What role do they play in the energy budget of the interstellar medium? Are they galactic or also extragalactic? The cosmic ray particles, at least up to about 10^{15} eV, are considered of galactic origin and shock waves of expanding supernovae remnants are ideal candidates to supply the power for their acceleration. Evidences supporting this hypothesis have recently been reported by AGILE and Fermi, with the observation of gammas presumably coming from neutral pion emission from accelerated protons in the Supernova Remnant W44 [2, 3] and SR IC 443 [4], by Cherenkov imaging telescopes [5] and in X-ray emissions from the borders of SRN [6]. The accelerated particles are injected into the interstellar space, where they remain about 10^7 years before escaping into the intergalactic space. This long period is due to their coupling to the galactic magnetic field and to scattering on random magnetic fields that leads to a random walk in real space (diffusion) and momentum space (diffusive reacceleration). Diffusion provides a high degree of isotropy for the cosmic rays, however the random nature (in space and time) especially of nearby recent SNRs could produce the small anisotropy observed at Earth [7]. Particles are also spatially convected away by the galactic wind, inducing adiabatic losses and lose energy when they interact with interstellar matter or, especially for electrons, with the electromagnetic field and radiation of the Galaxy by synchrotron radiation and inverse Compton scattering. New particles and spallation products are obtained by interaction of cosmic rays with the interstellar matter. Solar modulation affects the low energy part of the cosmic

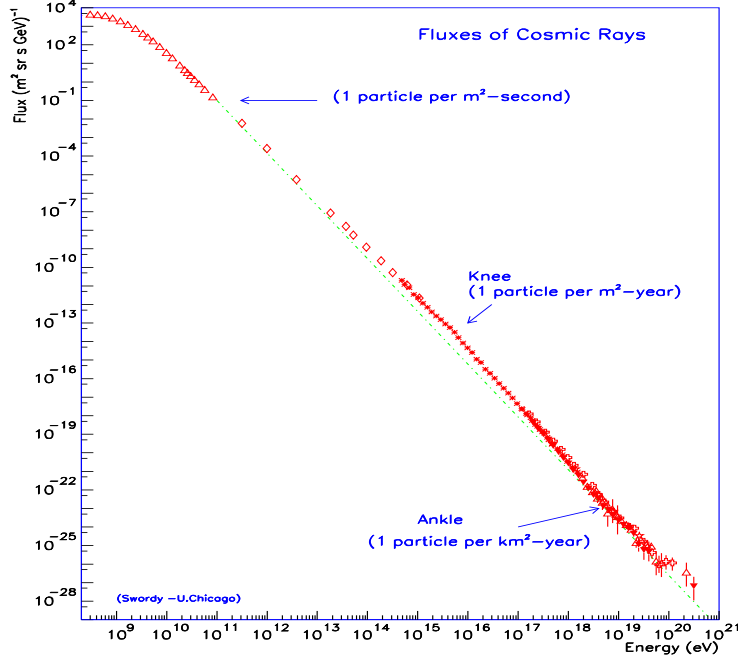


Figure 1: All particle cosmic ray energy spectrum. Figure from [1]

rays and plays an important role in the precise determination of the cosmic ray interstellar energy spectrum. Understanding the origin, acceleration and propagation of cosmic rays in the Galaxy requires the combination of many different investigations over a wide range of energy, including chemical composition, anisotropy, and solar modulation.

2. Cosmic rays elemental composition

The experimental methods divide the cosmic ray energy spectrum in two large intervals. The first, below the first knee, is explored by direct measurements, carried out by experiments on stratospheric balloons or in space on board satellites or International Space Station, with single particle identification and energy definition. The second one, over the knee, where the low particle flux makes feasible only indirect observations, is measured by very large on ground detectors and the particle nature is inferred, on basis of the statistics and with considerable systematic uncertainties, studying their interaction with the atmosphere. The experimental observation of a change of slope, or “knee”, in the cosmic ray flux at 10^{15} eV energy scale has not yet found an explanation universally accepted, after almost half a century since its discovery. According to some theoretical models, the knee is linked to the process of acceleration of cosmic rays. In case of acceleration due to shock waves of expanding supernovae remnants, the existence of a maximum rigidity $R = pc/(Ze)$, p being the momentum of a particle of charge Ze , is predicted, to which the mechanism of acceleration becomes inefficient. In this scenario, the spectrum of each individual element in primary cosmic rays would show a “cutoff” at a characteristic momentum with a linear dependence on the atomic number Z . These models appear to be confirmed by experimental data that show a “knee” at $3 \div 5 \times 10^{15}$ eV presumably due to light primary masses cutoff [8, 9] and, very recently, another at 8×10^{16} eV attributed to heavy primary nuclei [10]. Therefore, the observed inclusive spectrum would be the superposition of individual spectra, weighted with the relative abundances of the elements in the flux of the primaries and the knee would reflect the different composition of cosmic rays. An alternative explanation of the knee is adopted by models that relate it to leakage of cosmic rays from the Galaxy. In this case the knee is expected to occur at lower energies for light nuclei as compared to heavy ones, due to the rigidity-dependence of the Larmor radius of cosmic rays propagating in the galactic magnetic field [11].

In this paper we deal with direct measurements of cosmic rays under the “knee”, with a focus on the chemical composition that provides important information about cosmic ray primary sources, secondary production, acceleration and propagation processes through the interstellar medium. An extensive work has been conducted in space and at the top of the atmosphere in the energy region between few GeV/n and hundreds of TeV/n, starting with

the pioneer series of Proton satellite experiments of Grigorov [12], extended, later, by the JACEE [13] and RUNJOB [14] balloon-borne experiments and by HEAO [15] and SOKOL [16] on board satellites and CRN [17] on board the Space Shuttle. At present new data are released by ATIC [18], BESS [19], CREAM [20], TRACER [21], PPB-BETS [22] as results of Long Duration Balloon flights in Antarctica and by PAMELA on satellite. Very precise measurement of nuclei at the TeV region are expected by AMS-02 [23], operating outside the ISS since May 2011. The most precise data on proton and helium energy spectra have been achieved by PAMELA [24] between 1 GeV and 1.2 TeV for protons and 1 GeV/n to 500 GeV/n for helium and by CREAM [20] between 2.5 TeV and 250 TeV for protons and 630 GeV/n to 63 TeV/n for helium. Results from different experiments [13, 14, 18, 19, 20, 24, 25, 26, 27, 28] up to 10 TeV/n, multiplied by $E^{2.7}$, are shown in Fig. 2. The extrapolation to higher energy of the PAMELA fluxes suggests a good agreement with those published by CREAM and JACEE [13] but they are higher than the RUNJOB [14] helium data. PAMELA data show a spectral hardening, at 230-240 GV, which appears present also in the ATIC2 data [18]. For long time a tantalizing question has focused on the possible uniqueness of the index spectrum for all nuclei, including protons. It has been difficult to prove subtle differences between the different spectra, because spectral indices determined by different measurements performed over a limited energy range or with low statistics and large background contamination could not provide a definite answer. The PAMELA data, taken over a wide energy range above the atmosphere, show clearly this difference between the proton and helium slopes, as seen in Fig. 3, where the ratio of the fluxes is presented as a function of rigidity. In this configuration the possible impact of systematic errors is reduced, because several instrumental effects cancel in the ratio. The proton-to-helium flux ratio shows a continuous and smooth decrease and it is well described by a power law down to rigidities as low as 5 GV with a spectral index of 0.1. The data are compared with Zatsepin model [29]. The energy spectra of the most abundant heavy nuclei [15, 17, 21, 30] are presented in Fig. 4. The agreement among the different experiments appears to be quite good in the regions of the overlaps. The insufficient precision of the measurements does not allow to observe a significant trend of the spectral indices with Z charge. Energy power laws with an average spectral index of 2.65 ± 0.05 fit well all the TRACER data above 20 GeV [21]. This behavior suggests a common origin of all cosmic ray species. However, protons and helium data advise for a more careful analysis. In fact, it is expected that the

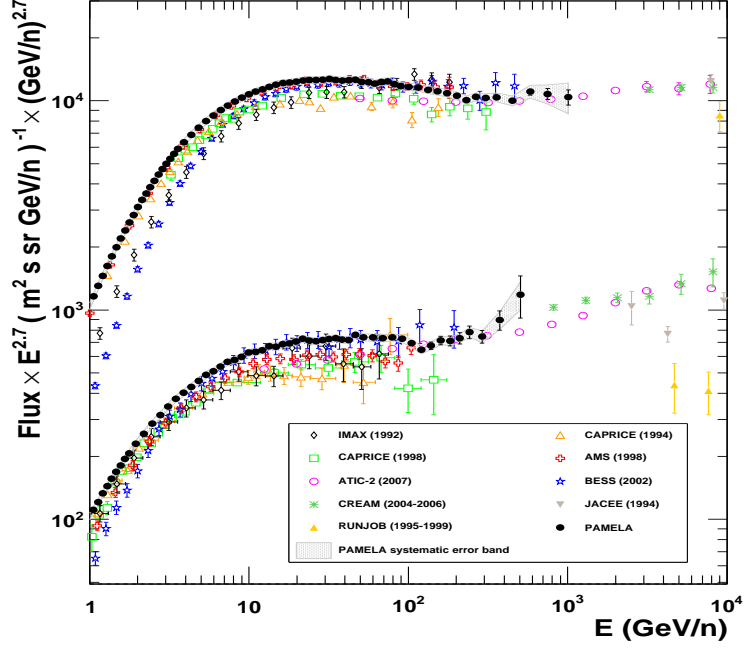


Figure 2: Proton and helium absolute fluxes measured between 1 GeV/n and 10 TeV/n: JACEE [13], CAPRICE 1994 [25], AMS-01 [27], IMAX [26], CAPRICE 1998 [28], BESS [19], RUNJOB [14], ATIC-2 [18], PAMELA [24], CREAM [20]. The measurements have been obtained by balloon-borne experiments but AMS-01 and PAMELA.

competing action of physical escape from the Galaxy, which depends on energy, and loss by spallation in the interstellar medium (ISM), which depends on the nuclear charge Z (or more correctly, on atomic number A), should lead to some changes in the spectral shape for the different nuclei that would be difficult to describe by the same power-law spectrum. Moreover, a recent accurate analysis [32] of direct measurements of the energy spectra of the major mass components of cosmic rays indicates the presence of an 'ankle' in the region of several hundred GeV/n. The ankle, which varies in magnitude from one element to another, is much sharper than predicted by cosmic ray origin models in which supernova remnants are responsible for cosmic ray acceleration and it appears as a new, steeper component is necessary.

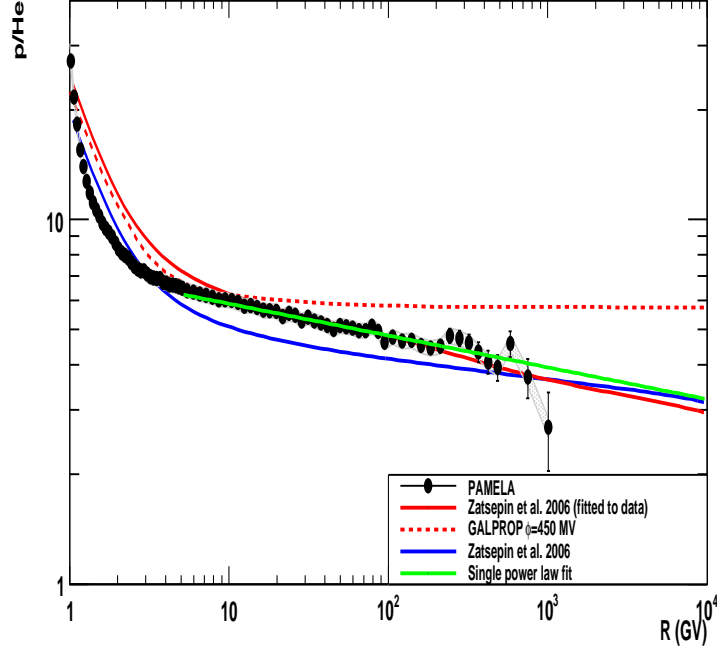


Figure 3: Ratio between proton and helium data of PAMELA vs. Rigidity. The shaded area represents the estimated systematic uncertainty. Lines show the fit using one single power law (describing the difference of the two spectral indices), the GALPROP calculation and the Zatsepin models using the original values of the paper [29] and fitted to the data.

2.1. Cosmic ray secondaries

The combined effect of acceleration and propagation of cosmic rays in the Galaxy leads to a difference between the spectra at the source and those measured at Earth. Secondary nuclei are produced by spallation in the interaction of primary nuclei with interstellar matter. Powerful tools to characterize the diffusion property of the ISM and to test the propagation models are therefore the measurements of the abundances and energy spectra of secondary elements such as Boron, Beryllium and Lithium and, particularly, the ratios between secondary and primary cosmic ray fluxes as B/C, Be/C, Li/C etc. They are directly connected to the crossed amount of matter in the Galaxy and to the nuclei lifetime before escaping from the Galaxy. Actually, the energy dependence of the B/C ratio is directly connected with the

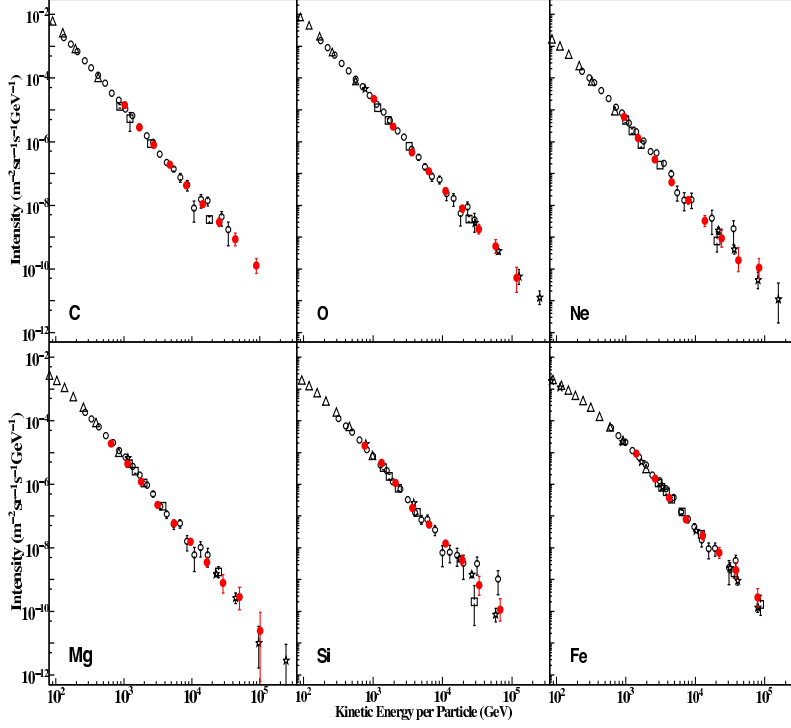


Figure 4: Energy spectra of the more abundant heavy nuclei. Results of CREAM-II [30] (filled circles), HEAO [15] (triangles), CRN [17] (squares), ATIC [31] (open circles) and TRACER [21] (stars). Figure from [30].

diffusion coefficient, or more in general with the escape time, which scales as the inverse of the coefficient if diffusion is the only process responsible for escape. The results of measurements of the B/C ratio performed by several experiments [15, 31, 33, 34, 35, 36] are shown in Fig. 5, that includes also an extrapolation (dotted line) for an $E^{-0.6}$ decrease of this ratio with energy, inferred from measurements at low energy. However, this energy dependence would imply too small values for the escape path length of cosmic rays at the highest energies and a large anisotropy of cosmic rays at knee would be measured. Thus, it is quite interesting that the more precise data of TRACER [33] on the B/C ratio above 100 GeV/nucleon, and also, as shown in Fig. 5, some of the results of other measurements, appear to lie above the $E^{-0.6}$ prediction. This feature may suggest that the energy dependence of the escape path length flattens at high energy, and perhaps indicates an

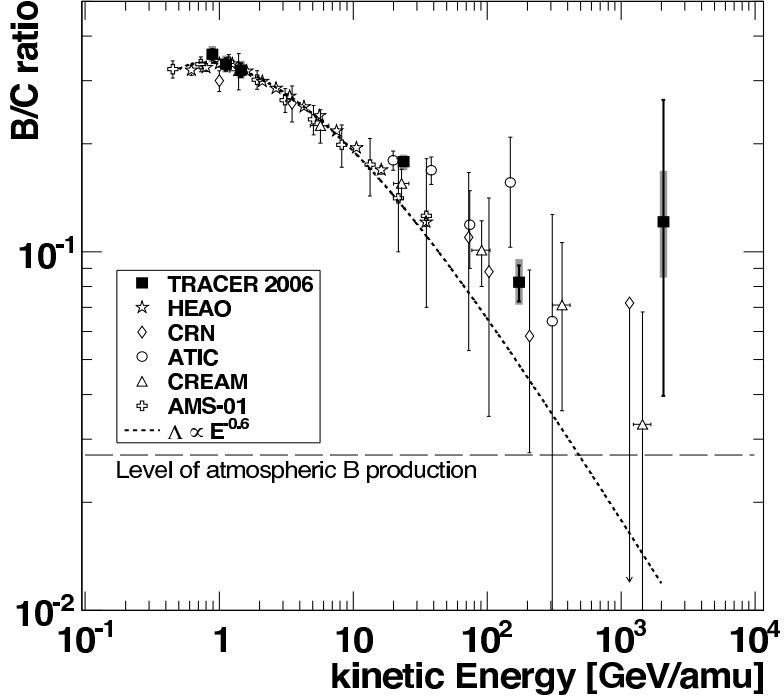


Figure 5: The boron-to-carbon abundance ratio as a function of kinetic energy per nucleon. Error bars are statistical (thin) and systematic (thick). A model corresponding to an escape path length $E^{-0.6}$ (dotted) is shown. The level of atmospheric production of boron (dashed) is indicated. HEAO [15], TRACER [33], CRN [34], ATIC [31], CREAM [35] and AMS-01 [36]. Figure from [33].

asymptotic transition to a constant residual path length. On the other hand, if this transition exists one should expect the appearance of a feature in the all-particle spectrum which does not seem to be there. In the next months, the AMS-02 space mission will allow for fundamental improvements to the understanding of the origin and propagation of cosmic rays in the Galaxy. New results at higher energy will be provided by CALET experiment [37] planned to be installed outside the ISS in 2014.

3. High energy cosmic-ray electrons

Electrons (and positrons) constitute about 1% of the total cosmic-ray flux. While small, this component provides important information regarding the origin and propagation of cosmic rays in the Galaxy that is not accessible from the study of the cosmic-ray nuclear components due to their differing energy-loss processes. In fact, because of their low mass, electrons undergo severe energy losses through synchrotron radiation in the Galactic magnetic field and inverse Compton scattering with the interstellar radiation fields and the cosmic microwave background radiation.

There are two possible origins of high-energy electrons in the cosmic radiation: primary electrons accelerated at sources such as SNR and secondary electrons produced by processes such as nuclear interactions of cosmic rays with the interstellar matter. From an energetic point of view it was realized already in the fifties (e.g. [38]) that supernovae explosions released sufficient energy to power the cosmic rays in the Galaxy. Evidence for synchrotron X-ray emission [39, 40] strongly supports the hypothesis that Galactic cosmic-ray electrons originate in supernovae. In this case, TeV gamma rays should be produced via the inverse Compton process between accelerated electrons and the cosmic microwave background radiation and indeed TeV gamma rays were detected (e.g. [41]).

Secondary electrons originate from the interaction of cosmic rays, mostly protons and helium nuclei, on the interstellar matter (hydrogen and helium). In this process positrons are produced too. Since the interaction involves positively charged particles, charge conservation implies that slightly more positrons than electrons are created (e.g. [42]). Since the observed positron component is of the order of ten percent and less of the electron one above a few GeV (e.g. [43]), the majority of electrons must be of primary origin. However, additional sources of electrons (and positrons) cannot be excluded. The recent observation by the PAMELA satellite of a rising positron fraction up to ~ 100 GeV [44], later confirmed by the Fermi experiment [45] up to 200 GeV, has prompted a considerable effort in the theoretical interpretation of the data. New sources ranging from astrophysical objects such as pulsars, e.g. [46], or more exotic sources such as dark matter particles, e.g. [47], have been proposed to explain the results. Similarly, the recent measurement of an excess in the “all electron” ($e^- + e^+$) spectrum by the ATIC collaboration [48] at a few hundred GeV has been interpreted in terms of a dark matter signal or a contribution of a nearby pulsar.

Because of energy losses via synchrotron radiation and inverse Compton scattering, the lifetime of high energy electrons is approximately: $2.5 \times 10^5(\text{yr})/E(\text{TeV})$ [49]. In diffusion models for transport of cosmic rays in the Galaxy this implies a short range propagation scale (~ 1 kpc) for high energy electrons, hence local sources are expected to play an important role (e.g. [49, 50, 51]). Furthermore, a small number of sources well localized in space may induce features in the spectral shape of the electron energy spectrum [51, 52] and anisotropies in the arrival direction of very high energy electrons (e.g. [49]). However, Delahaye et al. [51] noted that a full relativistic treatment of the energy losses smooths the global spectral shape significantly reducing the peaking structures resulting from using the Thomson approximation of the inverse Compton energy losses.

3.1. The “all-electron” spectrum

Detection of high-energy electrons has been conducted over the years employing the particle cascades produced by electrons in calorimeters. Such approach provides sufficient energy resolution and acceptance to extend the measurement of the electron spectrum beyond 1 TeV. However, negative particles cannot be straightforwardly separated from positive ones, hence the energy spectrum refers to the sum of $e^- + e^+$ (i.e. “all-electron”).

As previously noted, recently the balloon-borne experiment ATIC reported an excess of galactic cosmic-ray electrons at energies between 300-800 GeV [48]. The excess appeared as a structure in the all-electron energy spectrum with a sharp cutoff around 620 GeV, which was interpreted in terms of contribution of a nearby astrophysical object such as pulsar or dark matter signal. The same energy region was originally probed by the balloon-borne experiment by Kobayashi et al. [53] and later on by the balloon-borne experiment PPB-BETS [22], by the satellite-borne experiment Fermi [54, 55] and by the atmospheric Cherenkov experiment H.E.S.S. [56, 57]. Figure 6¹ shows these measurements. It can be noted that the recent measurements by Fermi and H.E.S.S. are consistent with ATIC results within statistical and systematic uncertainties but neither confirms this structure in the spectrum.

¹As commonly done, the figures in this paper show the fluxes multiplied by E^3 , where E is the energy in GeV. Reducing the decades of variation of the flux, this allows for a clearer picture of the spectral shapes. However, this implies that the absolute energy uncertainties are added to the flux uncertainties.

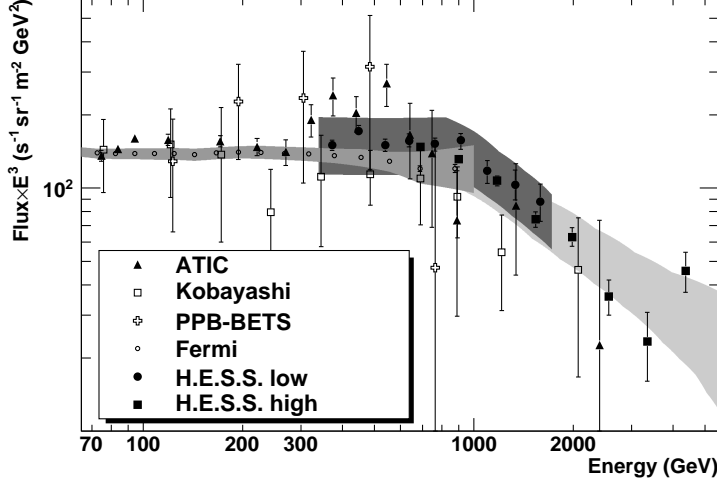


Figure 6: The all-electron energy spectrum measured by Kobayashi[53], PPB-BETS [22], ATIC [48], H.E.S.S. [57, 56] and Fermi [54]. The shaded areas indicate the systematic uncertainties in the Fermi and H.E.S.S. results (two sets of data measurements for H.E.S.S.).

All these measurements required powerful particle identification to separate electrons from a vast background of protons and heavier nuclei. The identification was based upon calorimetry information (in the H.E.S.S. case the calorimeter was the atmosphere itself) such as energy losses and shower development. Thickness of the employed calorimeter as well as validity of simulations are fundamental ingredients for a reliable hadron rejection and corresponding systematic uncertainties. Moreover, atmospheric secondaries, i.e. produced by interaction of cosmic rays with the residual atmosphere above the payload, comprise an irreducibly contamination for balloon-borne experiments. These secondary electrons (and positrons) can only be estimated by Montecarlo or analytical calculations. Furthermore, since they approximately maintain the spectral shape of the parent cosmic rays, their contamination increases as the energy increases amounting often to 10% or more of the signal in the hundred GeV region (e.g. see [22]).

Additional sources of discrepancies arise from efficiency and energy determinations. Selection efficiencies are an experimental challenge since they require a very good knowledge of the detector performances during data taking. Often, to reduce the systematic uncertainties, the selection efficiencies

are derived from flight data, but a fully unbiased cross calibration of the efficiencies in flight is quite impossible and simulations have to be used. The simulations are usually validated by comparisons with test-beam data, which do not account for the flight condition, and, whenever possible, flight data. However, unproven assumption have to be made resulting in uncertainties that have to be included in the results. It has to be noted that efficiency uncertainty usually affects the absolute normalization of the fluxes and have a smaller impact on the shape of the spectra.

The shaded areas in Fig. 6 shows the systematic uncertainties in the Fermi and H.E.S.S. measurements. In the case of Fermi they account for uncertainties in the estimation of the hadronic background. However, these uncertainties do not account for those deriving from the energy determination. For the experiments in Fig. 6, the energy was obtained by measuring the development of the electromagnetic cascade in the calorimeter. Also in this case the thickness of the calorimeter plays a significant role in the precision of the measurement with an energy resolution ranging from $\sim 15\%$ for Fermi to $\sim 3\%$ for ATIC at few hundred GeV.

In the case of H.E.S.S. the shaded areas indicate the approximate systematic uncertainties arising from the modeling of hadronic interactions and of the atmosphere. The energy scale can approximately shift of 15%. It should be mentioned that the energy determination strongly depends on simulations since experimental calibration at beam test cannot be performed, differently from space and balloon-borne experiments. Additionally, a contamination by the diffuse γ -ray background affects the H.E.S.S. results, estimated at a level of 10% even if a significantly larger contamination of $\simeq 50\%$ cannot be excluded [57]. It has to be noted that the presence of this contamination implies that the H.E.S.S. electron spectrum is probably an upper limit of the real spectrum and that the contamination, due to the different spectral shapes of electrons and diffuse γ -rays, is energy dependent, hence potentially affecting the shape of the spectrum.

The effect of systematic uncertainties can be understood also looking at Fig. 7 that shows the ratio between the all-electron spectra measured by Fermi [54] using two different event selections: one is the standard analysis published in [55], the other uses a significantly smaller set of events ($\sim 5\%$ of the total) that crossed at least 12 radiation lengths in the calorimeter (see [54] for more details). The energy resolution of this second set of events is significantly better: about 3%-5% between 100 GeV and 1 TeV. Considering that, on top of the statistical errors, the systematic uncertainties are

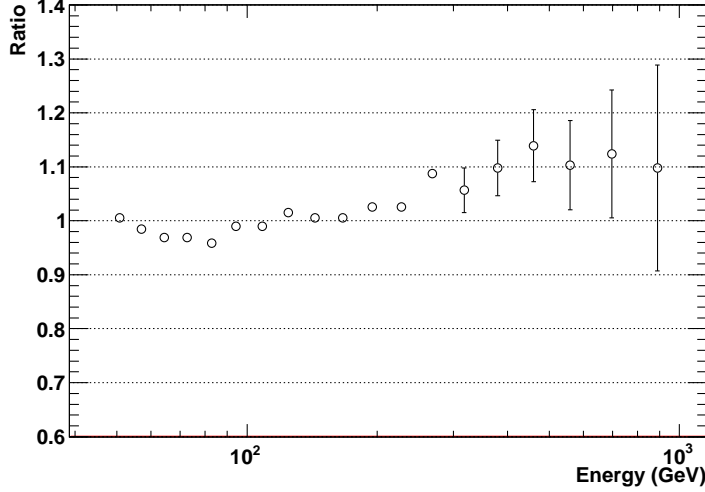


Figure 7: The ratio between the all-electron spectra measured by Fermi [54] using two event selections with different energy resolution (fluxes with better resolution divided by the ones with lower resolution).

$\sim 5\%$, increasing as the energy increases and without accounting for the absolute energy uncertainty (see Fig. 6), the two results are perfectly consistent. However, it can also be noticed that the spectrum obtained with the higher energy resolution is systematically higher than the one with larger statistics above 200 GeV. This is another confirmation that a detailed interpretation of the electron data require a careful analysis of the experimental data including all statistical and systematic uncertainties. It also points to the need for more precise measurements.

As can be seen from Fig. 6, the “all electron” spectrum is well represented by a single power law of about -3 of spectral index up to ~ 1 TeV, above which energy a cutoff like feature is present. A combination of contributions from a limited number of nearby sources and distant ones uniformly distributed appears consistent with the experimental results as shown in Fig. 14 of [51]. However, as discussed, taking into account all experimental uncertainties spectral features in the hundred GeV region cannot be excluded.

3.2. The e^- spectrum

It has been often noted, e.g. [51], that the separate cosmic-ray e^- and e^+ fluxes yield much more information and provide stronger constraints to

theoretical models than the all-electron spectrum. Since the first detection of cosmic-ray e^- in the early sixties [58], several experiments were performed to measure this component. Figure 8 left shows the e^- energy spectrum measured by recent cosmic-ray experiments [59, 60, 61, 62, 63] (the highest data point from HEAT [62] refer to the sum of electrons and positrons). and a

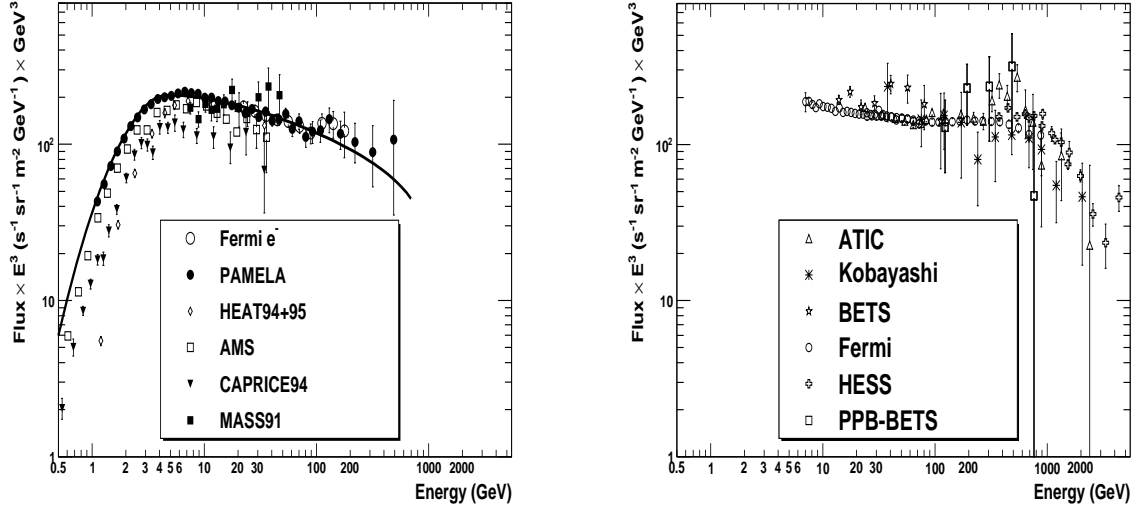


Figure 8: Left: recent measurements of the cosmic-ray e^- energy spectrum: CAPRICE94 [60], HEAT [62], AMS [61], MASS91 [63], PAMELA [59] and Fermi [45]. The solid line is a theoretical calculation based on the GALPROP code [64]. Right: the all-electron energy spectrum measured by Kobayashi[53], BETS [65] PPB-BETS [22], ATIC [48], H.E.S.S. [57, 56] and Fermi [54].

theoretical calculation of the e^- spectrum based on the GALPROP code [64]. The calculation (solid line) was performed using a spatial Kolmogorov diffusion with spectral index $\delta = 0.34$ and diffusive reacceleration characterized by an Alfvén speed $v_A = 36$ km/s, the halo height was 4 kpc (parameters from [66]). The resulting flux was normalized to PAMELA data at ~ 70 GeV. For the secondary e^- production during propagation it used primary proton and helium spectra reproducing the corresponding measured PAMELA spectra [24] and it was calculated for solar minimum, using the force field approximation [67] ($\Phi = 600$ MV). As a comparison the Figure 8 right shows measurements of the all-electron spectrum [22, 48, 53, 54, 56, 57, 65] with the same energy scale.

Differences in the data at low energies are mostly due to the effect of solar modulation for the various data taking periods. Therefore, here we will mostly discuss measurements of electrons with energies above 10 GeV, for which these effects are much less significant.

Especially the PAMELA and Fermi results show a rather smooth energy dependence of the energy spectra in a relatively good agreement with the GALPROP calculation except at higher energies where all experimental spectra are harder. Such hardening can be explained with additional leptonic components with a hard spectrum (e.g. [51, 54]), which, contributing equally to electrons and positrons, would likewise explain the increase in the positron fraction measured by PAMELA [44]. The spectral flattening can be as well reproduced by standard cosmic-ray models by adjusting the injection spectrum at the source; however, these models cannot explain the PAMELA positron data. A possible solution was proposed by Blasi [68], Ahlers et al. [69] and Fujita et al. [70] that considered the production and acceleration of secondary electrons and positrons by hadronic interactions of the accelerated protons in SNR shock waves. With such assumption, they were able to fit the Fermi (and H.E.S.S.) electron data and, at the same time, reproduce the PAMELA positron fraction. It should be mentioned that GALPROP does not fully describe cosmic-ray electron propagation. This calculation is commonly used assuming a continuous distribution of sources in the Galaxy. However this does not seem plausible for primary high energy electrons, since, as previously discussed, this assumption should only hold for a relatively close neighborhood. Furthermore, as pointed out in [71], there is a higher concentration of SNRs in the spiral arms of the Galaxy, therefore one should consider an inhomogeneous source distribution.

As in the case of the very-high-energy all-electron spectrum the interpretation of the results depends on the precision of the measurements. Especially systematic uncertainties, often larger than statistical errors, have to be properly taken into account in any data interpretation. However, it is very difficult to correctly estimate systematic uncertainties. An excellent approach to their determination resides in comparing measurements taken with different apparatus. For example, we compared PAMELA electron spectrum to the Fermi all-electron spectrum. For this comparison, we constructed a PAMELA all-electron spectrum using the PAMELA e^- data [59] and positron fraction [72]. Figure 9 shows the Fermi and PAMELA all-electron spectra up to 100 GeV, i.e. the highest energy bin for which the PAMELA collaboration presented the positron fraction. The PAMELA spectrum appears softer than the Fermi

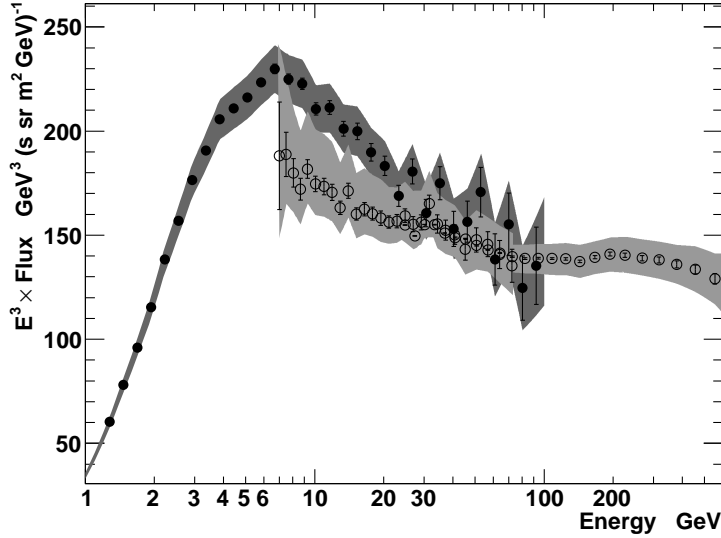


Figure 9: The all ($e^- + e^+$) electron energy spectrum from Fermi [54] (open circles) and PAMELA [59, 72] (full circles).

one, however the two spectral indexes differ by less than a standard deviation (-3.17 ± 0.07 for PAMELA and -3.112 ± 0.002 for Fermi) when fitting the data with a single power-law from 30 to 100 GeV and accounting only for statistical errors. At lower energies, the electron flux measured by PAMELA is higher (about 20% at 10 GeV) than that measured by Fermi. Considering that the data were collected partially over the same period of time the differences cannot be ascribed to solar modulation. However, systematic uncertainties, indicated as shaded areas in Fig. 9, account for most of the differences. Once more this illustrates why systematic uncertainties cannot be neglected when modelling experimental results.

Recently the Fermi collaboration published data on e^- and e^+ fluxes [45] where the two species were distinguished up to 200 GeV using the opposite distortion of the Earth's shadow caused by Earth's magnetic field. These results are particularly interesting not only because they confirm the PAMELA positron results but also because the differences between the Fermi and PAMELA e^- spectra are significantly reduced respect to the comparison discussed above (Fig. 9). Figure 10 shows the e^- spectrum measured by Fermi compared with the one by PAMELA [59] along with single power-law fits to

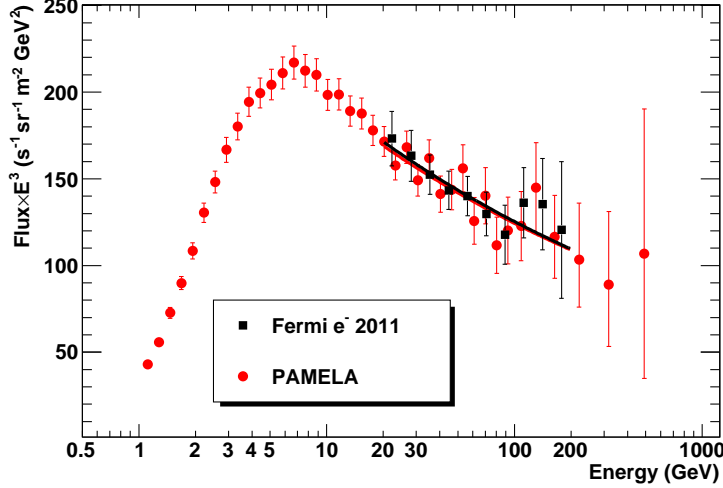


Figure 10: The e^- energy spectrum measured by Fermi [45] and PAMELA [59]. The solid lines are single power-law fit to the data between 20 and 200 GeV (red: PAMELA, black: Fermi). For both measurements the error bars include both statistical and systematic uncertainties quadratically summed and these were the errors considered by the fitting procedures.

the data between 20 and 200 GeV. An excellent agreement can be noticed: there are negligible differences in the absolute values and in the two spectral index (-3.19 ± 0.04 for PAMELA and -3.20 ± 0.08 for Fermi). Apparently, the better agreement between PAMELA and Fermi electron spectra is due to improved instrument response functions used in the Fermi data (see [45]). This agreement can be used to reduce the effect of systematic uncertainties, providing an e^- spectrum more precise than each single measurement. It is interesting to note that both PAMELA and Fermi e^- spectra harden and hint to a structure around 100 GeV not unlike a similar feature noticeable in the ATIC all-electron spectrum (see Fig. 6).

3.3. Future

Experiments based on atmospheric Cherenkov telescopes such as H.E.S.S. and the future CTA [73] are very important for studies of the Galactic cosmic-ray electron spectrum since they are able to probe the TeV energy region with orders of magnitude larger collection areas than balloon- and satellite-borne experiments. However, the uncertainties related to hadronic and dif-

fuse γ -ray backgrounds and to the energy determinations significantly overshadow the statistical uncertainties muddling the interpretation of the measurements. The authors believe that a direct measurement of the cosmic-ray electron spectrum is still the preferable approach also in the high-energy region. Future experiments such as the space-borne CALET and Gamma-400 and balloon-borne CREST may provide the needed precision for a significantly improved understanding of the cosmic-ray electron spectrum, their propagation and origin.

CALET [37] is an experiment designed to measure the all-electron cosmic ray spectrum from 1 GeV to 20 TeV. The apparatus is built around a 30 radiation length calorimeter and it will be placed on board the International Space Station (ISS) sometime around 2014. With an acceptance of about $0.12 \text{ m}^2\text{sr}$, CALET will significantly extend previous electron measurement with a significant improvement on the systematic uncertainties.

A similar calorimetry approach will be employed by the Gamma-400 [74] experiment. This experiment is aimed to study the high-energy gamma-ray flux and cosmic-ray electrons and nuclei. The apparatus will be placed on board a Russian satellite, which launch is foreseen for 2017-2018. With a similarly deep but significantly larger calorimeter (acceptance of about $1 \text{ m}^2\text{sr}$), Gamma-400 should be able to extend the cosmic-ray measurements performed by CALET.

A different approach has been proposed for the CREST experiment [75] that aims to detect the synchrotron photons generated at x-ray energies by TeV cosmic-ray electrons in the Earth's magnetic field. While affected by a relatively poor energy resolution, the experiment, sensitive to electrons of energies greater than 2 TeV, can efficiently sample the multi-TeV region. The apparatus, carried on a long duration balloon-flight², will be able to observe up to 30 electrons with energy greater than 2 TeV in a 2 week flight [75].

As previously pointed out, separate data of positrons and electrons provide stronger grounds to any interpretation of the cosmic-ray electron data. Till now the e^- spectrum has been measured up to 600 GeV thanks to the PAMELA data [59] but with limited statistics. However, more precise data can be expected in the future. In fact, on the 19th of May 2011 the AMS-02 apparatus [23] was installed onboard the ISS and it started collecting data.

²An engineering flight of CREST took place in 2009 [76], a long duration balloon flight has not yet been scheduled.

The apparatus is equipped with a permanent magnet, a silicon tracking device, an electromagnetic calorimeter, a Transition Radiation Detector and a Ring Imaging Cherenkov detector. Similar in scope to the PAMELA experiment, AMS has a significantly larger acceptance (about a factor 20) and additional particle identifier detectors such as a Transition Radiation that will provide a significant improvement in statistics and systematics respect to PAMELA. Considering the 10-year long AMS mission, the experiment may be able to provide sufficiently precise results to search for structures in the electron spectrum at least up to 1 TeV.

4. Acknowledgments

We would like to thank the PAMELA Collaboration for providing some of the information included in this paper and E. Mocchiutti for helping in the production of several figures.

References

- [1] J. Cronin, T. Gaisser, S. Swordy, *Sci. Amer.* 276 (1997) 44.
- [2] A. Giuliani, et al., *Astrophys. J.* 742 (2011) L30.
- [3] A. A. Abdo, et al., *Science* 327 (2010) 1103.
- [4] M. Tavani, et al., *Astrophys. J. Lett.* 710 (2010) L151.
- [5] S. Funk, *Adv. Space Res.* 41 (2008) 464.
- [6] J. Vink, in: *Proc. The X-ray Universe (Madrid, 2005)*, p. 319.
- [7] P. Blasi, E. Amato, *arXiv:1105.4529*, 2011.
- [8] T. Antoni, et al., *Astropart. Phys.* 16 (2002) 373.
- [9] T. Antoni, et al., *Astropart. Phys.* 24 (2002) 1.
- [10] W. D. Apel, et al., *Phys. Rev. Lett.* 107 (2011) 171104.
- [11] J. R. Hörandel, *Astropart. Phys.* 21 (2004) 241.
- [12] N. L. Grigorov, et al., in: *Proc. 12th Int. Cosmic Ray Conf. (Hobart, 1971)*, volume 5, p. 1746.
- [13] K. Asakimori, et al., *Astrophys. J.* 502 (1998) 278.
- [14] M. Hareyama, et al., *J. of Phys.: Conference Series* 31 (2006) 159.
- [15] J. J. Engelmann, et al., *Astr. Astrophys.* 233 (1990) 96.
- [16] I. P. Ivanenko, et al., in: *Proc. 23rd Int. Cosmic Ray Conf. (Calgary, 1993)*, volume 2, p. 17.
- [17] D. Müller, et al., *Astrophys. J.* 374 (1991) 356.

- [18] J. P. Wefel, et al., in: Proc. 30th Int. Cosmic Ray Conf. (Merida, 2007), volume 2, p. 31.
- [19] S. Haino, et al., Phys. Lett. B 594 (2004) 35.
- [20] Y. S. Yoon, et al., Astrophys. J. 728 (2011) 122.
- [21] M. Ave, et al., Astrophys. J. 678 (2008) 262.
- [22] S. Torii, et al., arXiv:0809.0760, 2008.
- [23] R. Battiston, et al., in: Proc. 29th Int. Cosmic Ray Conf. (Pune, 2005), volume 10, p. 151.
- [24] O. Adriani, et al., Science 106 (2011) 201101.
- [25] M. Boezio, et al., Astrophys. J. 518 (1999) 457.
- [26] W. Menn, et al., Astrophys. J. 533 (2000) 281.
- [27] J. Alcaraz, et al., Phys. Lett. B 490 (2000) 27.
- [28] M. Boezio, et al., Astropart. Phys. 19 (2003) 583.
- [29] V. I. Zatsepin, N. V. Sokolskaya, Astron. Astrophys. 458 (2006) 1.
- [30] P. Maestro, et al., Nucl. Phys. Proc. Suppl. 196 (2009) 239.
- [31] A. D. Panov, et al., in: Proc. 30th Int. Cosmic Ray Conf. (Merida, 2007), volume 2, p. 3.
- [32] A. D. Erlykin, A. W. Wolfendale, Astropart. Phys. 35 (2011) 371.
- [33] A. Obermeier, et al., Astrophys. J. 742 (2011) 14.
- [34] S. P. Swordy, et al., Astrophys. J. 349 (1990) 625.
- [35] H. S. Ahn, et al., Astropart. Phys. 30-3 (2008) 133.
- [36] M. Aguilar, et al., Astrophys. J. 724 (2010) 329.
- [37] S. Torii, et al., in: Proc. 32nd Int. Cosmic Ray Conf. (Beijing), volume 6, p. 344.

- [38] V. L. Ginzburg, S. I. Syrovatskii, *The Origin of Cosmic Rays*, New York: Macmillan, 1964.
- [39] K. Koyama, R. Petre, E. V. Gotthelf, U. Hwang, M. Matsuura, M. Ozaki, S. S. Holt, *Nature* 378 (1995) 255.
- [40] G. E. Allen, et al., *Astrophys. J. Lett.* 487 (1997) L97.
- [41] F. Aharonian, et al., *Nature* 432 (2004) 675.
- [42] T. Kamae, N. Karlsson, T. Mizuno, T. A. and T. Koi, *Astrophys. J.* 647 (2006) 692.
- [43] J. A. D. Shong, R. H. Hildebrand, P. Meyer, *Phys. Rev. Lett.* 12 (1964) 3.
- [44] O. Adriani, et al., *Nature* 458 (2009) 607.
- [45] M. Ackermann, et al., *Phys. Rev. Lett.* 108 (2012) 011103.
- [46] D. Malyshev, I. Cholis, J. Gelfand, *Phys. Rev. D* 80 (2009) 063005.
- [47] M. Cirelli, M. Kadastik, M. Raidal, A. Strumia, *Nucl. Phys. B* 813 (2008) 1.
- [48] J. Chang, et al., *Nature* 456 (2008) 362.
- [49] T. Kobayashi, Y. Komori, K. Yoshida, J. Nishimura, *Astrophys. J.* 601 (2004) 340.
- [50] F. A. Aharonian, A. M. Atoyan, H. J. Volk, *Astron. Astrophys.* 294 (1995) L41.
- [51] T. Delahaye, J. Lavalle, R. Lineros, F. Donato, N. Fornengo, *Astron. Astrophys.* 524 (2010) A51.
- [52] J. Nishimura, et al., *Astrophys. J.* 238 (1980) 394.
- [53] T. Kobayashi, J. Nishimura, Y. Komori, T. Shirai, N. Tateyama, T. Taira, K. Yoshida, T. Yuda, in: *Proc. 26th Int. Cosmic Ray Conf.* (Salt Lake City, 1999), volume 3, p. 61.
- [54] M. Ackermann, et al., *Phys. Rev. D* 82 (2010) 092004.

- [55] A. A. Abdo, et al., Phys. Rev. Lett. 102 (2009) 181101.
- [56] F. Aharonian, et al., Astron. Astrophys. 508 (2009) 561.
- [57] F. Aharonian, et al., Phys. Rev. Lett. 101 (2008) 261104.
- [58] J. A. Earl, Phys. Rev. Lett. 6 (1961) 125.
- [59] O. Adriani, et al., Phys. Rev. Lett. 332 (2011) 69.
- [60] M. Boezio, et al., Astrophys. J. 532 (2000) 653.
- [61] J. Alcaraz, et al., Phys. Lett. B 484 (2000) 10.
- [62] M. A. DuVernois, et al., Astrophys. J. 559 (2001) 296.
- [63] C. Grimani, et al., Astron. Astrophys. 392 (2002) 287.
- [64] A. W. Strong, I. V. Moskalenko, Astrophys. J. 509 (1998) 212.
- [65] S. Torii, et al., Astrophys. J. 559 (2001) 973.
- [66] V. S. Ptuskin, et al., Astrophys. J. 642 (2006) 902.
- [67] L. J. Gleeson, W. I. Axford, Astrophys. J. 154 (1968) 1011.
- [68] P. Blasi, Phys. Rev. Lett. 103 (2009) 051104.
- [69] M. Ahlers, P. Mertsch, S. Sarkar, Phys. Rev. D 80 (2009) 123017.
- [70] Y. Fujita, K. Kohri, R. Yamazaki, K. Ioka, Phys. Rev. D 80 (2009) 063003.
- [71] N. J. Shaviv, E. Nakar, T. Piran, Phys. Rev. Lett. 103 (2009) 111302.
- [72] O. Adriani, et al., Astropart. Phys. 34 (2010) 1.
- [73] The CTA Consortium, Exp. Astro. 32 (2011) 193.
- [74] A. M. Galper, et al., arXiv:1201.2490, 2012.
- [75] M. Schubnell, et al., in: Proc. 30th Int. Cosmic Ray Conf. (Merida, 2007), volume 2, p. 305.
- [76] S. Nutter, et al., in: Proc. 31st Int. Cosmic Ray Conf. (Łódź, 2009).